


Cite this: *RSC Adv.*, 2021, 11, 32981

# Improving the electrochemical performance of cathode composites using different sized solid electrolytes for all solid-state lithium batteries

Rajesh Rajagopal,<sup>ab</sup> Yuvaraj Subramanian<sup>a</sup> and Kwang-Sun Ryu  <sup>\*ab</sup>

We studied the efficiency of different particle-sized sulfide solid electrolyte-based cathode composites. First, we prepared the  $\text{Li}_7\text{P}_2\text{S}_8\text{I}$  solid electrolytes with different particle sizes through a high energy ball milling process and solution method. The structural details of the prepared solid electrolytes were studied by powder X-ray diffraction. The surface morphologies and particle size of the electrolytes were studied by field emission electron microscopy. The ionic conductivity of the prepared solid electrolytes was studied by the electrochemical impedance spectroscopy technique. Finally, we have prepared a  $\text{LiNi}_{0.8}\text{Co}_{0.1}\text{Mn}_{0.1}\text{O}_2$  (NCM 811) based cathode composite and studied the electrochemical performance of the fabricated all-solid-state lithium batteries. The mixed particle-sized solid electrolyte-based cathode composite exhibited higher specific capacitance ( $127.2 \text{ mA h g}^{-1}$ ) than the uniform-sized solid electrolyte-based cathode composite ( $117.1 \text{ mA h g}^{-1}$ ). The electrochemical analysis confirmed that the sulfide solid electrolytes with mixed particle size exhibited better electrochemical performance.

Received 4th August 2021  
Accepted 28th September 2021

DOI: 10.1039/d1ra05897e

rsc.li/rsc-advances

## 1. Introduction

Lithium-ion batteries (LIBs) systems are well-known energy storage systems due to their superior energy storage capacity, high energy and power densities, and are widely used in most advanced technology devices such as electric vehicles and portable electronic devices, smartphones, and laptop computers.<sup>1,2</sup> All solid-state lithium batteries (ASSBs) are a potential alternative to conventional liquid or polymer lithium-ion batteries as they are safer and have higher energy density. In addition, unlike conventional batteries, they have low flammability, and higher thermal stability.<sup>3</sup>

However, ASSBs are limited by the low ionic conductivity of the solid electrolytes (compared to liquid organic electrolytes) and electrode–electrolyte interface problems. These are significant problems that should be overcome before replacing the conventional lithium-ion batteries. Recently, numerous inorganic solid electrolytes with the ionic conductivity of  $10^{-3}$  to  $10^{-2} \text{ S cm}^{-1}$ , which is close to the liquid organic electrolytes have been proposed. They include sulfide, oxide, phosphide, nitride, and halide-based electrolytes. Among them, sulfide-based solid electrolytes have attracted greater interest due to their compatibility and high ionic conductivity. However, electrode–electrolyte interface problems remains a challenge even with the inorganic based ASSBs;<sup>4–6</sup> some inorganic solid

electrolyte reacts with electrode materials and produces by-products that rapidly degrade the battery performance. For instance,  $\text{Li}_{10}\text{GeP}_2\text{S}_{12}$  (LGPS) solid electrolyte exhibited a high ionic conductivity value of  $1.2 \times 10^{-2} \text{ S cm}^{-1}$  at room temperature, unfortunately, this LGPS solid electrolyte reacts with Li-metal anode resulting in poor electrochemical performance.<sup>7</sup> In addition, during the electrochemical reaction, a charge transfer occurs between the electrode–electrolyte through point-to-point contact. This kind of charge transfer enhances the electrode–electrolyte interfacial resistance resulting in poor cycle stability. To overcome these challenges, among others, researchers have suggested introducing conducting polymer layers on the lithium metal anode surface; this prevents the side reaction and increases contact between the Li-metal anode and solid electrolyte.<sup>8</sup> On the cathode side, a high conducting coating layer was introduced on the surface to reduce the interfacial resistance value. Several lithium metal oxides, such as  $\text{LiNbO}_3$ , and  $\text{Li}_2\text{ZrO}_3$  have been used as the coating material to reduce the interfacial resistance and increase the ASSBs performance.<sup>9,10</sup> Recently, mixed sizes of commonly used cathode materials were used to prepare a cathode composite which increases the contact between the electrode and electrolyte and reduces the interfacial resistance value.<sup>11</sup> Interestingly, Sakuda *et al.* prepared a cathode composite using a combination of different sizes of the commonly used cathode materials and solid electrolytes and studied the electrochemical performances.<sup>12</sup> In addition, mixed ionic and electronic conducting materials have also been used to increase the interfacial contact between the electrolyte and the electrode materials.<sup>13</sup> While sulfide offers outstanding performance benefits, to the

<sup>a</sup>Department of Chemistry, University of Ulsan, Doowang-dong, Nam-gu, Ulsan, 44776, Korea. E-mail: rryuks@ulsan.ac.kr; Fax: +82-52-712-8002; Tel: +82-52-712-8003

<sup>b</sup>Energy Harvest Storage Research Center (EHSRC), University of Ulsan, Mugeo-dong, Nam-gu, Ulsan, 44610, Korea


best of our knowledge, so far, mixed sizes sulfide solid electrolytes-based cathode composite has not been prepared. To further improve on the above, we hypothesized that mixed particle sizes-based sulfide solid electrolytes may improve the electrochemical performance of ASSBs.

In this study, we prepared a  $\text{Li}_7\text{P}_2\text{S}_8\text{I}$  glass-ceramic solid electrolyte using different particle sizes by ball mill method and wet chemical process. The crystalline nature and the particle size of the solid electrolytes were studied by powder X-ray diffraction (XRD) technique and FESEM analysis. Then different sizes of  $\text{Li}_7\text{P}_2\text{S}_8\text{I}$  solid electrolytes were used to prepare a cathode composite for the fabrication of ASSBs. Additionally, we evaluated the efficiency of the mixed-sized solid electrolytes-based composite and compared it with the uniform-sized solid electrolytes-based cathode composite. The mixed-sized solid electrolytes-based cathode composite exhibited higher specific capacity value than uniform-sized solid electrolytes-based cathode composite.

## 2. Experimental

First,  $\text{Li}_7\text{P}_2\text{S}_8\text{I}$  solid electrolyte was prepared through high-energy wet ball milling. Briefly, 0.6895 g of  $\text{Li}_2\text{S}$  (99.98%, Sigma Aldrich), 1.1113 g of  $\text{P}_2\text{S}_5$  (99%, Sigma Aldrich), and 0.6645 g of  $\text{LiI}$  (99%, Sigma Aldrich) were ground into fine powder for 15 minutes using mortar and pestle. Then the fine powder was transferred to an alumina ball mill vessel (80 ml), with 25 zirconia balls (10 mm diameter). Then, about 10 ml of *n*-heptane was added to the above mixture and the container was sealed to prevent air exposure. Then the ball mill vessel was brought out from the glove box and fixed to the ball-milling machine (Pulverisette, Fritsch). The ball mill reaction was carried at 400 rpm for 12 h. During the ball milling process, after every 30 min of milling, there was a 15 min rest and the rotation direction was changed to avoid overheating and good mixing. After the milling process, the resultant product was transferred to a Petri dish and dried at 100 °C in a glove box for 12 h to completely remove the heptane. Finally, the fine powder was heat-treated at 160 °C for 3 hours to obtain glass ceramic material. The resultant glass-ceramic solid electrolyte was named  $\text{Li}_7\text{P}_2\text{S}_8\text{I}$  (LPSI). The same process was repeated within 24 hours and the resultant product was named as s $\text{Li}_7\text{P}_2\text{S}_8\text{I}$  (sLPSI). The  $\text{Li}_7\text{P}_2\text{S}_8\text{I}$  solid electrolyte was prepared by wet chemical process. Briefly, 0.6895 g of  $\text{Li}_2\text{S}$ , 1.1113 g of  $\text{P}_2\text{S}_5$ , and 0.6645 g of  $\text{LiI}$  were ground into fine powder using mortar and pestle. Then, the powder was dispersed in 40 ml of anhydrous acetonitrile and stirred overnight. The resultant slurry was vacuum dried at 70 °C for 3 hours and the dry powder was heat-treated at 160 °C for 3 hours to obtain a glass ceramic material. The resultant glass-ceramic solid electrolyte was named w $\text{Li}_7\text{P}_2\text{S}_8\text{I}$  (wLPSI).

Cathode composite was prepared by mixing the active material ( $\text{LiNi}_{0.8}\text{Co}_{0.1}\text{Mn}_{0.1}\text{O}_2$ , NCM811), solid electrolyte, and super-P with the weight ratio of 70 : 28 : 2 with mortar and pestle. The above mixture was ground for 15 minutes and pelletized by hydraulic pressure. Again, the pellet was ground for 15 minutes and this process was repeated three times to

obtain a homogenous cathode composite. A schematic diagram for the cathode composite preparation process is shown in Fig. 1. To evaluate the effect of the particle size, prepared the cathode composite with different combinations of solid electrolytes particle size. Table 1 shows the weight ratio of solid electrolytes, active material, and conducting agent for the preparation of cathode composite.

The crystalline nature of the material was studied using Rigaku-Ultima (IV) X-ray diffractometer ( $K\alpha = 1.5418 \text{ \AA}$ ) within the  $2\theta$  range of 10 to 80° with the step size of 0.01 s<sup>-1</sup>. During the analysis, the solid electrolyte powder was protected from air and moisture exposure with an air-tight XRD holder at argon atmosphere. The ionic conductivity of the prepared  $\text{Li}_7\text{P}_2\text{S}_8\text{I}$  solid electrolytes was studied by electrochemical impedance spectroscopy (EIS) using Biologic SP 300. For the EIS measurement, the solid electrolyte was pressured into 10 mm diameter (~1.5 mm thickness) and the indium foil was attached on both sides for good electrical contact between the electrolyte and the electrode. The surface morphology and particle size of the prepared solid electrolytes were analyzed by field emission scanning electron microscope coupled with an EDS instrument (FE-SEM, JSM-7610F, Japan). For the galvanostatic charge-discharge analysis, we have prepared a 2032-type coin cell in an argon-filled glove box. For the fabrication of ASSB, 0.2 g of LPSI solid electrolyte was pressed into a pellet (16 mm diameter and ~1 mm thickness). Then 20 mg of the cathode composite was spread over one side of the solid electrolyte and covered with indium foil then pressed with 30 MPa. Pre-prepared, 60 mg of Li-In alloy anode material was uniformly spread over another surface of the solid electrolyte and pressed with 30 MPa, and assembled as 2032 – type coin cell.<sup>10</sup>

## 3. Results and discussion

The crystalline structure and phase of the prepared solid electrolytes were studied using powder XRD; the corresponding XRD patterns are shown in Fig. 2a. The prepared LPSI, sLPSI, and wLPSI solid electrolytes exhibited almost the same X-ray diffraction pattern. The characteristic peaks were observed at  $2\theta = 14.5^\circ, 18.0^\circ, 20.8^\circ, 24.5^\circ, 27.7^\circ, 29.0^\circ, 30.3^\circ, 31.7^\circ, 33.2^\circ, 36.6^\circ, 38.4^\circ, 41.1^\circ, 42.4^\circ, 44.1^\circ, 45.3^\circ, 46.5^\circ, 47.6^\circ, 49.3^\circ$  and  $55.2^\circ$ . The observed XRD pattern matched with the reported  $\text{Li}_7\text{P}_2\text{S}_8\text{I}$  solid electrolyte.<sup>14</sup> Further, we noticed that increased ball milling duration (24 hours) slightly decreased the crystalline nature (wide characteristic peaks) compared to 12 hours ball milling process. There were no obvious changes except the peak intensity variation after using the wet chemical synthesis method. The calculated ionic conductivity value of the prepared solid electrolytes is shown in Fig. 2b. From the EIS analysis, we observed that the LPSI solid electrolyte exhibited high ionic conductivity value of 1.23 mS cm<sup>-1</sup>. Increasing the ball milling time slightly decreased the ionic conductivity to 1.07 mS cm<sup>-1</sup> due to the increasing amorphous nature. The solid electrolyte prepared from wet chemical method exhibited the ionic conductivity value of 0.16 mS cm<sup>-1</sup> which was very close to the reported values.<sup>15,16</sup> For comparison, we also measure the ionic conductivity value of LPSI/sLPSI and LPSI/wLPSI solid



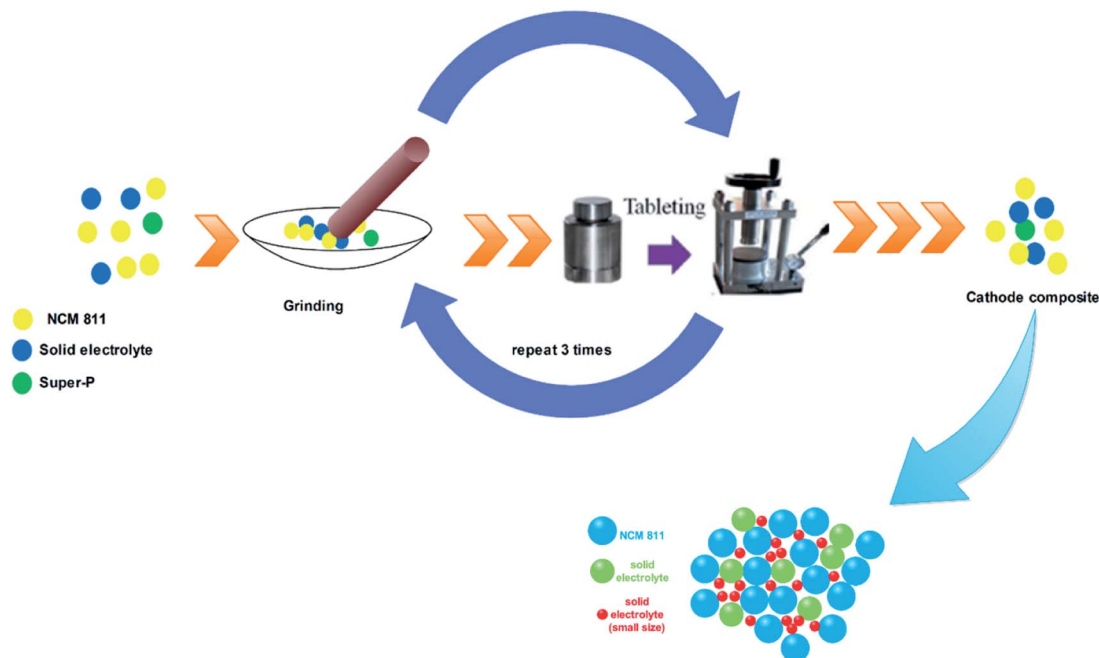


Fig. 1 The schematic diagram for the cathode composite preparation process.

electrolyte. Before the measurement, the solid electrolytes were mixed and ground for 30 minutes using mortar and pestle to ensure the proper mixing. The calculated ionic conductivity value of LPSI/sLPSI and LPSI/wLPSI solid electrolyte is 1.20 and  $0.42 \text{ mS cm}^{-1}$ , respectively. The obtained values are reliable and confirm the good mixing. Fig. 3(a–f) shows the FESEM images of LPSI, sLPSI, and wLPSI solid electrolytes with different magnifications. The particle size of the LPSI solid electrolyte prepared by high-energy ball mill process was in the range of 1 to  $10 \mu\text{m}$  and presented with many cracks over the surface. While the particle size remained the same even after increasing the ball milling time to 24 hours (sLPSI), the ratio of the small-sized particles was high compared to the large-sized particles. The particle size of wLPSI solid electrolyte prepared by wet chemical less than  $1 \mu\text{m}$  and exhibited a smooth surface.

Fig. 4 shows the FESEM images of the prepared cathode composites. From the FESEM analysis, we observed a uniform distribution of all the cathode composite components. The mixed particle-sized solid electrolytes are in close contact with the cathode material than uniform particle-sized solid electrolytes.<sup>17</sup>

Before the charge–discharge characteristic analysis, we have studied the ionic and electronic conductive performance of the

prepared cathode composite. For the ionic conductivity analysis, the prepared cathode composite ( $\sim 75 \text{ mg}$ ) was pelletized ( $\sim 250 \mu\text{m}$  thickness, 20 MPa) between the indium foil and the electrochemical impedance spectroscopy analysis was carried out between the frequency range of 7 MHz to 1 Hz. Fig. 5a shows the obtained Nyquist spectrum of the prepared cathode composite and we observed clear semicircles indicates the contact and interface resistance between the solid electrolyte and the cathode active material. The measured total resistance of the prepared LPSI, sLPSI, wLPSI, LPSI/sLPSI and LPSI/wLPSI solid electrolytes-based cathode composites are, 56.1, 54.6, 74.4, 46.4, and 59.9  $\Omega$ , respectively. As we expected, the measured total resistance value of the cathode composites following the trends of the electrolyte's ionic conductivity. Interestingly, sLPSI solid electrolyte based composite exhibited low resistance then LPSI solid electrolyte based composite due to its small particle size and good contact with electrode material. Similarly, we have measured the electronic conductivity value of the prepared cathode composites. For the electronic conductivity analysis, the prepared cathode composite ( $\sim 75 \text{ mg}$ ) was pelletized ( $\sim 250 \mu\text{m}$  thickness, 20 MPa) between the stainless steel and the chronoamperometry analysis was carried out for 600 s with the applied constant voltage of 1 V. Fig. 5b shows the obtained

Table 1 Materials composition (in weight) for the cathode composite preparation

Composite name	Solid electrolyte I (mg)	Solid electrolyte II (mg)	NCM 811 (mg)	Super-P (mg)
LPSI	168	—	420	12
sLPSI	168	—	420	12
wLPSI	168	—	420	12
LPSI/sLPSI	84	84	420	12
LPSI/wLPSI	84	84	420	12



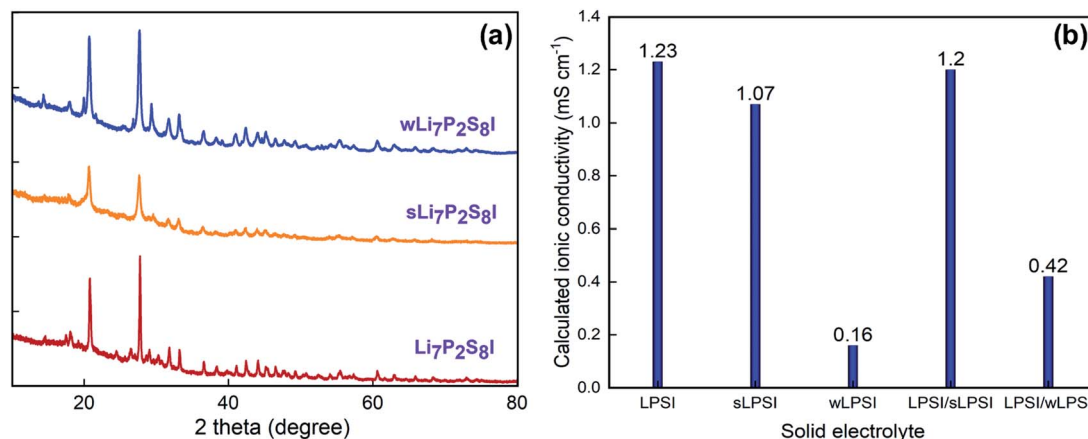


Fig. 2 (a) Powder X-ray diffraction pattern, and (b) calculated ionic conductivity value of LPSI, sLPSI, and wLPSI solid electrolytes and its mixers.

chronoamperometry graph of the prepared cathode composite and calculated electronic conductivity values are 0.30, 0.27, 0.10, 0.32 and 0.20  $\text{mS cm}^{-1}$  for LPSI, sLPSI, wLPSI, LPSI/sLPSI

and LPSI/wLPSI solid electrolytes-based cathode composites, respectively. We performed electrochemical impedance spectroscopy and charge-discharge analysis to study the

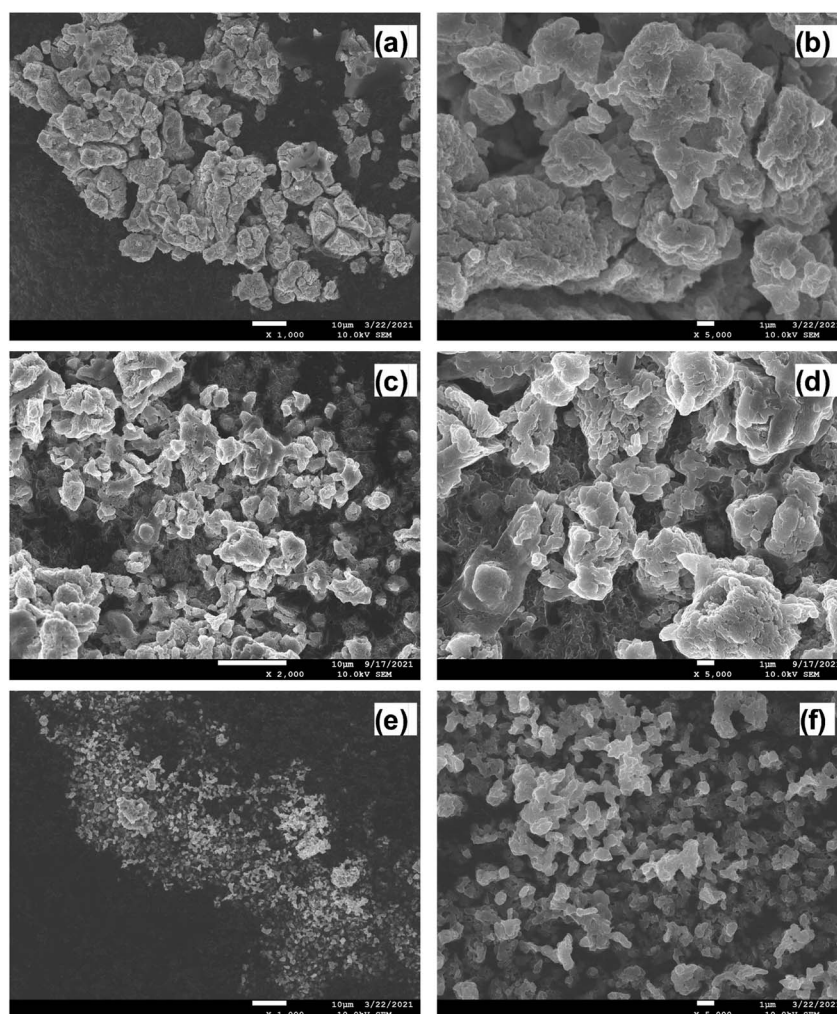


Fig. 3 FESEM images of (a and b) LPSI, (c and d) sLPSI, and (e and f) wLPSI solid electrolytes at different magnifications.



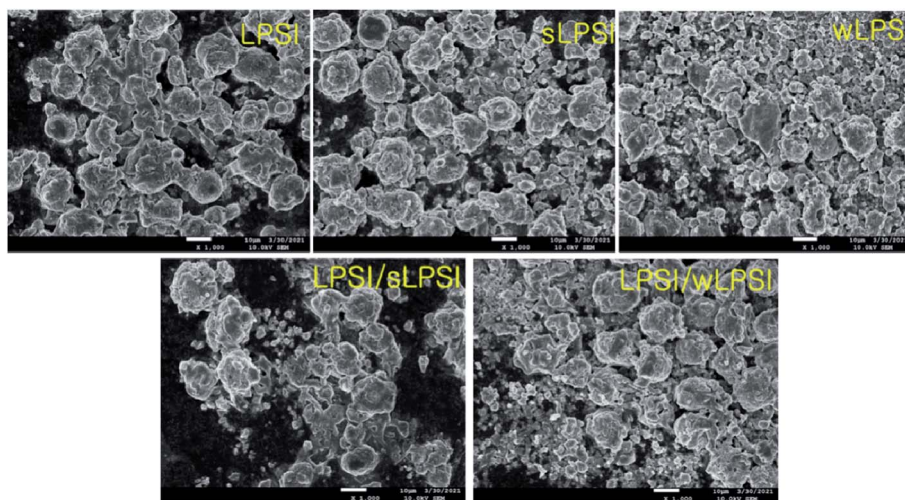


Fig. 4 FESEM images of cathode composites with different particle-sized solid electrolytes.

electrochemical performance of the prepared cathode composites. First, electrochemical impedance analysis was carried out in the frequency range of 7 MHz to 1 Hz to study the resistive and capacitive nature of the fabricated all-solid-state lithium battery. Fig. 5c and d shows the Nyquist plot of the Li-In/Li<sub>7</sub>P<sub>2</sub>S<sub>8</sub>I/NCM 811 composite asymmetric cell. The total resistance of the LPSI solid electrolyte-based cathode composite was 41 Ω, while increasing the ball milling time decreased the resistance value to 31.5 Ω (sLPSI based composite) due to the

increased number of small sized-solid electrolyte particles. On the other hand, the wLPSI solid electrolytes were in close contact with NCM 811 cathode material and exhibited high resistance (517 Ω) due to low ionic conductivity. As we expected, LPSI/sLPSI solid electrolyte-based cathode composite exhibited a decreased resistance value of 30.1 Ω and was in close contact with the cathode material. The measured resistance value of LPSI/wLPSI solid electrolyte was 51 Ω, which was significantly lower than wLPSI based cathode composite.

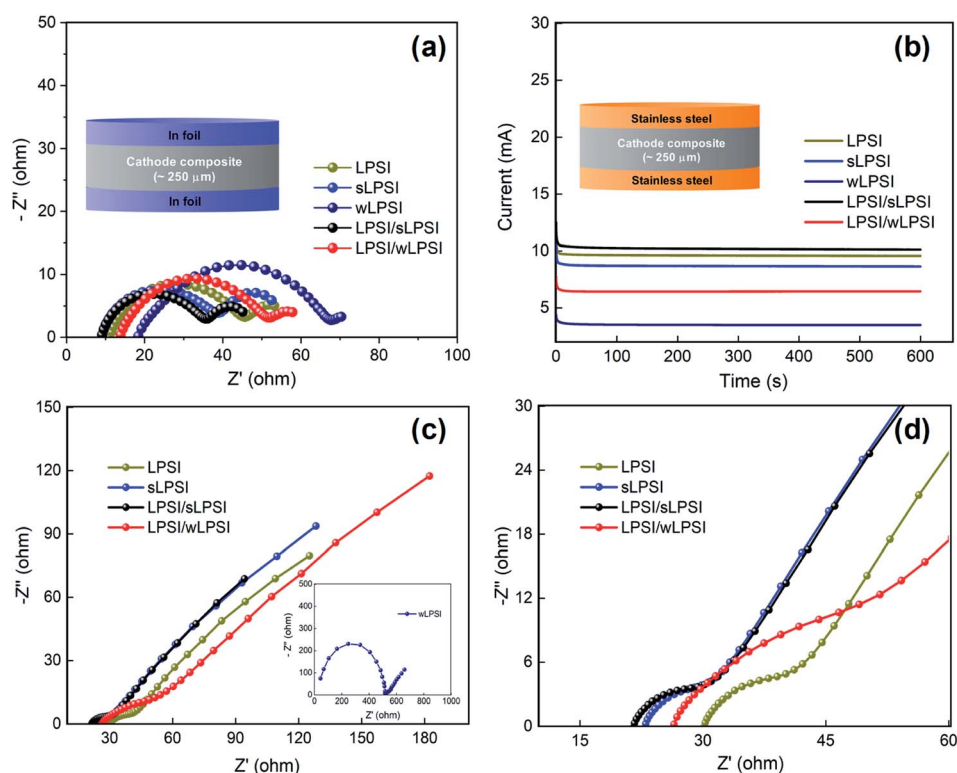


Fig. 5 (a) Nyquist plot, (b) chronoamperometry graph, of different particle-sized solid electrolytes, (c) and (d) Nyquist plot of all the fabricated solid-state lithium batteries with different particle-sized solid electrolyte-based cathode composites.

Finally, we performed a galvanostatic charge–discharge analysis of Li–In/Li<sub>7</sub>P<sub>2</sub>S<sub>8</sub>I/NCM 811 composite asymmetric cell with a potential of 2.38 V to 3.68 V at the current density of 15 mA g<sup>−1</sup> (0.1 C). The charge–discharge curve of the prepared all-solid-state lithium batteries are shown in Fig. 6a. The fabricated LPSI/sLPSI solid electrolyte-based ASSB exhibited a higher specific capacity value (127.2 mA h g<sup>−1</sup>) than those of LPSI (117.1 mA h g<sup>−1</sup>) and sLPSI (106.0 mA h g<sup>−1</sup>) solid electrolytes based all-solid-state lithium batteries. This could be because the mixed particle-sized solid electrolytes reduced the voids between the solid electrolyte and the NCM 811 cathode material. In addition, the close contact between the solid electrolytes and cathode material increased the lithium-ions conduction pathways and reduced the interfacial contact resistance at the electrolyte–electrode interface. Thus, the specific capacitance value of the mixed-sized solid electrolytes-based cathode composite is higher than the uniform-sized cathode composite.<sup>18,19</sup> The small particle-sized solid electrolytes-based cathode composite also exhibited good contact between the solid electrolyte and cathode material and but showed reduced specific capacity values (sLPSI = 106 mA h g<sup>−1</sup> and wLPSI = 79.9 mA h g<sup>−1</sup>) due to its low ionic conductivity. Unfortunately, LPSI/wLPSI mixed particle-sized solid electrolyte-based ASSB exhibited a low specific capacity value of 98.7 mA h g<sup>−1</sup>. Interestingly, the over voltage of the wLPSI solid electrolyte-based ASSB is much higher than all other ASSB. The particle size and ionic conductivity difference of wLPSI solid electrolyte is too far from all other solid

electrolytes, we believed that this could be the reason for high over voltage. In addition, we analyzed up to 50 cycles of the charge–discharge cycle stability and the corresponding graph is shown in Fig. 6b. Based on the cycle stability analysis, all the fabricated all-solid-state lithium batteries showed good stability even after 50 cycles. Similarly, we plot the coulombic efficiency and specific capacity retention of the fabricated ASSBs and shown in Fig. 6c and d, respectively. From Fig. 6c, we observed that the solid electrolytes prepared by ball mill process were exhibited almost same specific capacity retention due to its high ionic conductivity. Interestingly, the ionic conductivity of wLPSI solid electrolyte is much lower than other prepared solid electrolytes; the specific capacity retention value of wLPSI solid electrolyte based ASSB is higher than all other ASSBs, this may be due to its uniform size and good contact with electrode materials. Further mixing this wLPSI solid electrolyte with LPSI solid electrolyte (prepared by ball mill process), the specific capacity retention value decreased; this is reasonable because the difference in particle size and ionic conductivity of wLPSI solid electrolyte and LPSI solid electrolyte is too far than other cathode composite mixtures. In Fig. 6d, we observed the fabricated LPSI/sLPSI solid electrolyte-based ASSB exhibited better coulombic efficiency than other ASSBs.

## 4. Conclusions

In this study, we prepared Li<sub>7</sub>P<sub>2</sub>S<sub>8</sub>I solid electrolytes with different particle sizes using different preparation techniques.

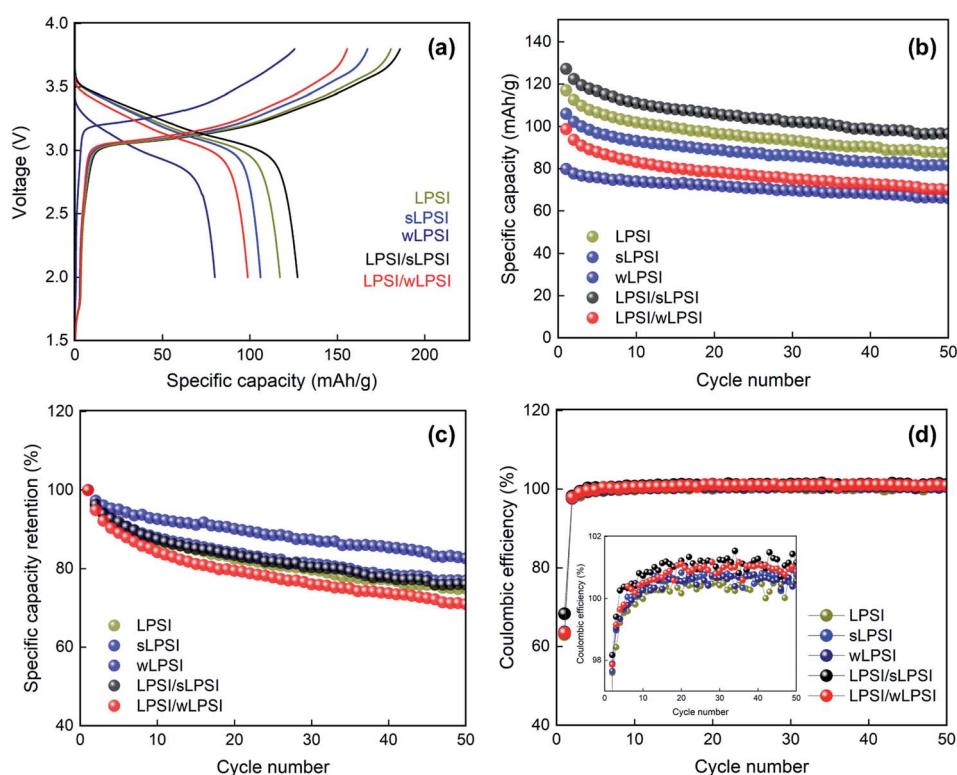


Fig. 6 (a) First cycle of charge–discharge graph, (b) charge–discharge cycle stability, (c) specific capacity retention, and (d) coulombic efficiency of all the fabricated solid-state lithium batteries with different particle-sized solid electrolyte-based cathode composites.



The solid electrolyte prepared by wet ball milling method exhibited a high ionic conductivity value. The particle sizes of the prepared solid electrolytes were measured using FESEM analysis. We fabricated cathode composites, using different particle sizes of the commonly used solid electrolyte materials. Interestingly, a mixture of LPSI and sLPSI solid electrolytes cathode composite exhibited a high specific capacity of 127.2 mA h g<sup>-1</sup> at the C-rate of 0.1 C. This suggests that the different particle sizes of the solid electrolytes helped to improve the contact between the solid electrolyte and cathode material and subsequently enhanced the electrochemical performances. This new concept provides an insight into a new method for the fabrication of more efficient all-solid-state lithium batteries.

## Conflicts of interest

There are no conflicts to declare.

## Acknowledgements

This study was supported by the National Research Foundation of Korea (NRF), funded by the Ministry of Education, Science, and Technology (MEST) of the Korean Government (NRF-2019R1A6A1A11053838).

## References

- 1 K. Hamabe, F. Utsuno and T. Ohkubo, Lithium conduction and the role of alkaline earth cations in Li<sub>2</sub>S–P<sub>2</sub>S<sub>5</sub>–MS (M = Ca, Sr, Ba) glasses, *J. Non-Cryst. Solids*, 2020, **538**, 120025.
- 2 X. Ruo-chen, X.-h. Xia, S.-h. Li, S.-z. Zhang, X.-l. Wang and J.-p. Tu, All-solid-state lithium–sulfur batteries based on a newly designed Li<sub>7</sub>P<sub>2.9</sub>Mn<sub>0.1</sub>S<sub>10.7</sub>I<sub>0.3</sub> superionic conductor, *J. Mater. Chem. A*, 2017, **5**(13), 6310–6317.
- 3 X. Zhenming, R. Chen and H. Zhu, A Li<sub>2</sub>CuPS<sub>4</sub> superionic conductor: a new sulfide-based solid-state electrolyte, *J. Mater. Chem. A*, 2019, **7**(20), 12645–12653.
- 4 C. Arthur V, S. M. Russell, D. R. Baker, K. J. Gaskell and K. Xu, In situ and quantitative characterization of solid electrolyte interphases, *Nano Lett.*, 2014, **14**(3), 1405–1412.
- 5 K. Takashi, H. Nakamura and S. Watano, Dry coating of electrode particle with model particle of sulfide solid electrolytes for all-solid-state secondary battery, *Powder Technol.*, 2018, **323**, 581–587.
- 6 Z. Jun, H. Zhong, C. Zheng, Y. Xia, C. Liang, H. Huang, Y. Gan, X. Tao and W. Zhang, All-solid-state batteries with slurry coated LiNi<sub>0.8</sub>Co<sub>0.1</sub>Mn<sub>0.1</sub>O<sub>2</sub> composite cathode and Li<sub>6</sub>PS<sub>5</sub>Cl electrolyte: Effect of binder content, *J. Power Sources*, 2018, **391**, 73–79.
- 7 Y. Kyungho, J.-J. Kim, W. M. Seong, M. H. Lee and K. Kang, Investigation on the interface between Li<sub>10</sub>GeP<sub>2</sub>S<sub>12</sub> electrolyte and carbon conductive agents in all-solid-state lithium battery, *Sci. Rep.*, 2018, **8**(1), 1–7.
- 8 S. Joscha, T. Günther, T. Knoche, C. Vieider, L. Köhler, A. Just, M. Keller, S. Passerini and G. Reinhart, All-solid-state lithium-ion and lithium metal batteries–paving the way to large-scale production, *J. Power Sources*, 2018, **382**, 160–175.
- 9 W. Felix, F. Strauss, X. Wu, B. Mogwitz, J. Hertle, J. Sann, M. Rohnke, T. Brezesinski and J. Janek, The Working Principle of a Li<sub>2</sub>CO<sub>3</sub>/LiNbO<sub>3</sub> Coating on NCM for Thiophosphate-Based All-Solid-State Batteries, *Chem. Mater.*, 2021, **33**(6), 2110–2125.
- 10 K. Young-Jin, R. Rajagopal, S. Kang and K.-S. Ryu, Novel dry deposition of LiNbO<sub>3</sub> or Li<sub>2</sub>ZrO<sub>3</sub> on LiNi<sub>0.6</sub>Co<sub>0.2</sub>Mn<sub>0.2</sub>O<sub>2</sub> for high performance all-solid-state lithium batteries, *Chem. Eng. J.*, 2020, **386**, 123975.
- 11 S. Florian, T. Bartsch, L. de Biasi, A.-Y. Kim, J. Janek, P. Hartmann and T. Brezesinski, Impact of cathode material particle size on the capacity of bulk-type all-solid-state batteries, *ACS Energy Lett.*, 2018, **3**(4), 992–996.
- 12 S. Atsushi, T. Takeuchi and H. Kobayashi, Electrode morphology in all-solid-state lithium secondary batteries consisting of LiNi<sub>1/3</sub>Co<sub>1/3</sub>Mn<sub>1/3</sub>O<sub>2</sub> and Li<sub>2</sub>S–P<sub>2</sub>S<sub>5</sub> solid electrolytes, *Solid State Ionics*, 2016, **285**, 112–117.
- 13 W. Chengwei, L. Zhang, H. Xie, G. Pastel, J. Dai, Y. Gong, B. Liu, E. D. Wachsman and L. Hu, Mixed ionic-electronic conductor enabled effective cathode-electrolyte interface in all solid state batteries, *Nano energy*, 2018, **50**, 393–400.
- 14 R. Ezhiylmurugan, Z. Liu, M. Gobet, K. Pilar, G. Sahu, W. Zhou, H. Wu, S. Greenbaum and C. Liang, An iodide-based Li<sub>7</sub>P<sub>2</sub>S<sub>8</sub>I superionic conductor, *J. Am. Chem. Soc.*, 2015, **137**(4), 1384–1387.
- 15 Y. Tokoharu, N. HuuHuyPhuc, H. Muto and A. Matsuda, Preparation of Li<sub>7</sub>P<sub>2</sub>S<sub>8</sub>I Solid Electrolyte and Its Application in All-Solid-State Lithium-Ion Batteries with Graphite Anode, *Electron. Mater. Lett.*, 2019, **15**(4), 409–414.
- 16 C. Seon-Joo, S.-H. Choi, A. D. Bui, Y.-J. Lee, S.-M. Lee, H.-C. Shin and Y.-C. Ha, LiI-doped sulfide solid electrolyte: enabling a high-capacity slurry-cast electrode by low-temperature post-sintering for practical all-solid-state lithium batteries, *ACS Appl. Mater. Interfaces*, 2018, **10**(37), 31404–31412.
- 17 C. Marcela, N. C. Rosero-Navarro, A. Miura and K. Tadanaga, Electrochemical performance of bulk-type all-solid-state batteries using small-sized Li<sub>7</sub>P<sub>3</sub>S<sub>11</sub> solid electrolyte prepared by liquid phase as the ionic conductor in the composite cathode, *Electrochim. Acta*, 2019, **296**, 473–480.
- 18 W. Hongli, J. P. Mwizerwa, X. Qi, X. Xu, H. Li, Q. Zhang, L. Cai, Y.-S. Hu and X. Yao, Nanoscaled Na<sub>3</sub>PS<sub>4</sub> solid electrolyte for all-solid-state FeS<sub>2</sub>/Na batteries with ultrahigh initial coulombic efficiency of 95% and excellent cyclic performances, *ACS Appl. Mater. Interfaces*, 2018, **10**(15), 12300–12304.
- 19 D. Mikaela R, S. T. King, K. J. Takeuchi, E. S. Takeuchi, L. Wang and A. C. Marschilok, Improved ionic conductivity and battery function in a lithium iodide solid electrolyte via particle size modification, *Electrochim. Acta*, 2021, 138569.

